The tympanic region of *Otaria byronia* (Otariidae, Carnivora) – morphology, ontogeny, age classes and dimorphism

C. M. Loza,[1] A. C. Scarano,[1,2,3] F. C. Galliari,[1,3] L. H. Soibelzon,[1,3] J. Negrete[4] and A. A. Carlini[1,3]

[1]*División Paleontología de Vertebrados, Museo de La Plata, Facultad de Ciencias Naturales y Museo, Universidad Nacional de La Plata, La Plata, Argentina*
[2]*Departamento de Ciencias Ambientales, Universidad Nacional de Avellaneda, Buenos Aires, Argentina*
[3]*Consejo Nacional de Investigaciones Científicas y Técnicas, Buenos Aires, Argentina*
[4]*Departamento de Biología de Predadores Tope, Instituto Antártico Argentino, Buenos Aires, Argentina*

Abstract

Here we describe and explore for the first time the ontogeny and sexual dimorphism of the auditory region of *Otaria byronia*. We studied the tympanic region of skulls of 237 specimens of different ages and sexes. Geometric morphometric methods were used to analyze the tympanic bulla. In addition, 3D reconstructions of the tympanic bulla were performed using computed tomography analysis scans and a serial wearing technique. We provide a description of the external and internal morphology of the tympanic bulla in both sexes and across different stages (bioclasses). The average shape of the bulla in *O. byronia* has a subtriangular contour, with variations between sexes and ages. Each stage (bioclasses I, II, and III) is characterized by the respective mean shape of the tympanic bulla and designated as a morphoclass (1, 2, and 3). In all cases, the ectotympanic shows greater surface area than the endotympanic, as in other otariids, in contrast to Phocidae. During ontogeny, the relative size of the ectotympanic increases, growing in all directions and covering the endotympanic. This pattern is seen to the greatest extent in adult males, in which the ectotympanic forms an extremely well-developed apophysis jugulare. No differences in internal morphology of the tympanic cavity were recorded between ages and sexes. The bulla does not increase in thickness in successive age classes; in fact, the walls are extremely thin in the adult stages, despite the extensive development of its processes. This pattern is opposite that observed in Phocidae. In morphoclass 3, adult males older than 7 years undergo hypermorphic change that results in a peramorphic condition when compared to adult females. These changes probably follow the same pattern shown by the rest of the skull and contribute to the marked sexual dimorphism of the species.

Key words: ontogeny; *Otaria byronia*; sexual dimorphism; South American sea lion; tympanic bulla.

Introduction

Since the pioneering papers of Van Kampen (1905) and Pocock (1921, 1922, 1929), the anatomy of the auditory bulla of Carnivora has been the focus of several studies (e.g. Van der Klaauw, 1930, 1931; Thenius, 1949; Hough, 1952; Ginsburg, 1966; Beaumont, 1968; Hunt, 1974; Arnaudo et al. 2014; Loza et al. 2015; Loza, 2016a), all within a descriptive and phylogenetic framework. Today the Carnivora are split into three main clades, Arctoidea, Aeluroidea, and Cynoidea, partially on the basis of auditory features such as the presence or absence of the septum bullae (Hough, 1948; Ivanoff, 2000). The Arctoidea (Flynn et al. 2005; Wozencraft, 1989, 2005) includes the Ursoidea (Ursidae + Hemicyonidae), the Musteloidea (Ailuridae, Mephitidae, Procyonidae, Mustelidae), and Pinnipedia, which are represented by three families: Otariidae (fur seals and sea lions), Odobenidae (walrus), and Phocidae (earless seals). Among pinnipeds, the morphology of the otic region of each main group seems to be related to the degree of aquatic adaptation. However, for most species of the group, the otic region has never been studied in detail.

The auditory region of pinnipeds has been briefly described for several Northern Hemisphere species (e.g.

Thenius, 1949; King, 1964; Odend'hal & Poulter, 1966; Gracham, 1967; Solnsteva, 1972, 1973a,b, 1975; Hunt, 1974; Nummela, 1995; Marsh, 2001; Berta et al. 2015), and few Southern Hemisphere ones (e.g. Wyss, 1987, 1988). Recently, Loza et al. (2015) presented a detailed description of the tympanic region in *Mirounga leonina* (Phocidae) compared with other phocid species (Loza, 2016a). In addition, some studies on hearing and audiometrics have been conducted on several Holarctic species (Mohl, 1967, 1968).

Several authors have also studied skull ontogeny and dimorphism in pinnipeds (e.g. King, 1983; Crespo, 1984; Cullen et al. 2014; Drehmer & Ferigolo, 1997; Brunner et al. 2004; Sanfelice & De Freitas, 2008; Tarnawsky et al. 2013, 2014); in particular, the tympanic region has been addressed in a comprehensive analysis of *M. leonina* (Phocidae) by Loza et al. (2015).

Here we describe and explore for the first time, the ontogeny and sexual dimorphism of the auditory region of the most dimorphic otariid, the South American sea lion, *Otaria byronia*, and characterize the otic region morphology of different age groups (= age classes). Finally, we compare it with the dimorphic southern elephant seal *M. leonina* (Phocidae) which has been studied recently (see Loza et al. 2015).

In addition to providing new data about this extant species, the analyses presented herein will contribute to the assessment and understanding of the past diversity of this clade. The fossil record of Otariidae is fragmentary, and diversity is frequently miscalculated because of the lack of tools reliably to accept or discard the validity of different nominal species based on fragments with variable morphology. Considering that the otic region is one of the portions of the skull that is frequently preserved in the fossil record (e.g. Wyss, 1987), we believe that this contribution will contribute to solving this issue. If this uncertainty about diversity (and its systematic context) is translated to phylogenetic analysis, the resulting phylogenies will not be close enough to reflect the true relationships between taxa.

Materials and methods

Specimen collection

The specimens studied are housed in the following institutions: AC: Cátedra de Anatomía Comparada, Facultad de Ciencias Naturales y Museo, Universidad Nacional de La Plata, La Plata, Buenos Aires, Argentina; FMM: Fundación Mundo Marino, San Clemente del Tuyú, Buenos Aires, Argentina; LAMAMA: Laboratorio de Mamíferos Marinos, Centro Nacional Patagónico, Consejo Nacional de Investigaciones Científicas y Técnicas, Puerto Madryn, Argentina; MACN: Museo de Ciencias Naturales Bernardino Rivadavia, Ciudad Autónoma de Buenos Aires, Buenos Aires, Argentina; MCN: Fundação Zoobotânica do Rio Grande do Sul, Porto Alegre, Brazil; MHNM: Museo de Historia Natural de Montevideo Montevideo, Uruguay; MLP: Colección de Mastozoología, Museo de La Plata, La Plata, Buenos Aires, Argentina; MMPma: Museo Municipal de Ciencias Naturales Lorenzo Scaglia, Mar del Plata, Buenos Aires,

Argentina; MNHN: Muséum National d'Historie Naturelle Collection de Anatomie Compareé, Paris, France; UDELAR: Facultad de Ciencias de Montevideo, Montevideo, Uruguay; UFSC: Universidade Federal de Santa Catarina, Florianópolis, Brazil; USNM: United States National Museum of Natural History, Smithsonian Institution, Washington DC, USA.

Absolute age and bioclasses

The tympanic regions of 237 complete skulls of *O. byronia* were studied (see Appendix 1). The terminology used in the description follows Laws (1953, 1993), Gray (1858), and Loza (2016a,b). For our morphometric analysis, 13 linear dimensions and five angles from the skull base and tympanic bulla were measured (Table 1, Fig. 1). In addition, the position and relative size of all foramina and apophyses were described for each skull, and compared with those of other otariids.

From the 237 skulls, the absolute ages of 87 individuals were estimated following a technique of counting dentin and cementum lines on tooth sections (described by Loza et al. 2016).

These 87 specimens were assigned to one of three age classes (here called bioclasses), which are defined by an age span, and characterized by diverse relevant biological and morphological criteria (e.g. sexual maturity, tooth eruption), obtained from several bibliographic sources (see Campagna, 1985; Crespo & Pedraza, 1991; Rosas et al. 1993; Grandi et al. 2009). A cross-validated procedure was conducted for the 87 specimens separated into the three bioclasses, and the resulting overall classification accuracy was 86% (Table 2). After the morphological analysis, we analyzed possible correspondence of these three bioclasses with ear morphology.

Bioclass I includes individuals from newborn up to 11 months old, sexually immature and dependent on maternal care, lacking or with partially erupted permanent dentition, sometimes with still-present deciduous teeth, and open tooth roots. The upper limit of this bioclass is coincident with the age when the animals take their first independent feeding journey (Vaz-Ferreira, 1981; Ponce de León & Pin, 2006; Canevari & Vaccaro, 2007).

Bioclass II comprises individuals between 1 and 4 years old, sexually immature but completely independent of maternal care, with fully erupted permanent dentition and closed tooth roots, except the canines, which are not fully grown and have open roots.

Bioclass III comprises individuals 5 years old or older, sexually mature, with either open or closed canine roots (the latter condition is only observed in old individuals).

Associated with the extreme sexual dimorphism present in *O. byronia* is a polygynous mating system in which adult males fight each other over harems of multiple females (more than six females) (Crespo, 1988). The lower age limit in which adult males enter these fights and are capable of winning (becoming alpha or dominant males) is approximately 7 years (Crespo, 1984; Crespo & Pedraza, 1991). Males younger than 7 years are reproductively active but usually lose these fights and remain restricted to peripheral positions outside the harems as peripheral males. For this reason, we also conducted a geometric morphometric analysis as described below, in which we grouped males older than 7 years separately from the remaining bioclass III individuals (adult females and adult males younger than 7 years). The category '7 years or more' included bioclass III individuals of known and unknown absolute age. The latter were incorporated using the minimum centroid size of the known absolute age of individuals with seven or more years as a threshold value: individuals of unknown age with centroid size

Table 1 Measurements and angles obtained from the skulls of *Otaria byronia*.

Measurement name	Definition
AA (anterior base angle)	Formed between the anterior surface of the bulla and the sagittal plane.
AJA (*apophysis jugulare* angle)	Formed between the axis that goes across its entire length and the sagittal plane.
AJL (length of *apophysis jugulare*)	Total length of this structure.
BGW (biglenoid width)	Distance between the external borders of the articular facets of both glenoid cavities.
BL (maximum length of the bulla)	Anteroposterior distance between the anterior-most point of the bulla (that is, behind the glenoid cavity, not considering apophyses or processes that may be scattered in front to the posterior limit of the glenoid cavity), and its posterior-most point (which is coincident with the triple suture between the ectotympanic, mastoids, and basioccipital).
BMW (bimastoid width)	Distance between the lateral-most extremes of the mastoid apophyses.
BW (maximum width of bulla)	Distance between the medial limit of the endotympanic and the external-most point of the *meatus acusticus externus*.
EcL (length of ectotympanic bone)	Distance between the anterior-most point of the ectotympanic and the posterior limit of the FSM.
EcW (ectotympanic width)	Distance between the endotympanic–ectotympanic suture and the lateral-most point of the ectotympanic tubercle.
EnL (maximum length of endotympanic bone)	Distance between the anterior-most point of the endotympanic and the FCP.
EnW (endotympanic width)	Distance between the medial limit of the endotympanic and the endotympanic–ectotympanic suture.
FJA (*foramen jugulare* angle)	Formed between the maximum diameter of the *foramen jugulare* (i.e. transversal) and the sagittal plane.
HFM (height of *foramen magnum*)	Maximum height of this structure.
LPA (posterior base angle)	Formed between the line that links the lateral-most point of the external acoustic meatus with the *foramen jugulare* (FJ) and goes across the posterior wall of the bulla, and the sagittal plane.
MA (medial base angle)	Formed between the medial surface of the bulla and the sagittal plane.
WFJ (width of *foramen jugulare*)	Maximum transversal diameter of this structure.
WM (width between meatuses)	Distance between the lateral-most extremes of the ectotympanic; on a level with the MAE.

values that were equal to or higher than this threshold were classified as being 7 years old or more.

Computed tomography (CT) scans were performed on two skulls of bioclass III specimens (see below), a male and a female, to investigate the internal three-dimensional structure of the tympanic bulla. CTs were obtained using a Scan Phillips Brilliance 64 with 0.56-mm slice thickness (*Z*-axis resolution), and 3D reconstructions were performed using MIMICS (10.01 version).

Additionally, to obtain more detailed data on the relationship between the endotympanic and ectotympanic bones, we performed a mechanical serial wear technique on three specimens of known age (one bioclass II, one male bioclass III, and one female bioclass III). The auditory regions were removed, embedded in synthetic resin, and serially worn with a metallographic polisher. Images were taken every 250 μm in the bioclass II specimen, and every 100 μm in both bioclass III specimens, using a Nikon Coolpix L120 digital camera. Afterwards, 3D reconstructions were performed using AMIRA (5.2.0. version, 2008).

Geometric morphometrics

For this study, we used 201 of the 237 studied skulls (36 were excluded because they are broken) (see Appendix 1), 87 of which had a known absolute age (114 of unknown age). Digital images in palatal view were obtained using a Nikon Coolpix L120 digital camera mounted on a stand. Each photograph included a ruler to

account for size in the analyses. The specimens were approximately equally distributed across sex classes and the three bioclasses were represented (Table 3). The 114 specimens of unknown age were assigned to a morphological age class (morphoclass) according to otic morphology (see below).

Geometric morphometric (GM) methods were used to analyze shape and size of the tympanic bulla in *O. byronia* (following Rohlf & Marcus, 1993; Adams et al. 2004, 2013; Zelditch et al. 2004). Two-dimensional coordinates of six homologous landmarks were digitized (Fig. 2): posteromedial contact between endotympanic and basioccipital (point 2); anteromedial contact between endotympanic and basisphenoid (point 5); most anteroventral point of the *meatus acusticus externus* where the retroarticular process of the glenoid cavity contacts the most anterolateral part of the ectotympanic (point 8): most posterior contact point between palatines (point 14); most lateral contact point between squamousal and jugal (point 15); the midpoint on anterior border of the foramen magnum or basion (point 16). Additionally, 10 equidistant semilandmarks (Gunz & Mitteroecker, 2013) were placed along the outline of the tympanic bulla to capture its shape and curvature (Fig. 2). The semilandmarks were slid along their tangent directions based on minimizing bending energy (Bookstein, 1996).

Landmarks were subjected to a generalized Procrustes analysis (GPA) (Rohlf & Slice, 1990). This procedure translates all specimens to the origin, scales them to unit centroid size, and optimally rotates them to minimize the total sums-of-squares deviations of
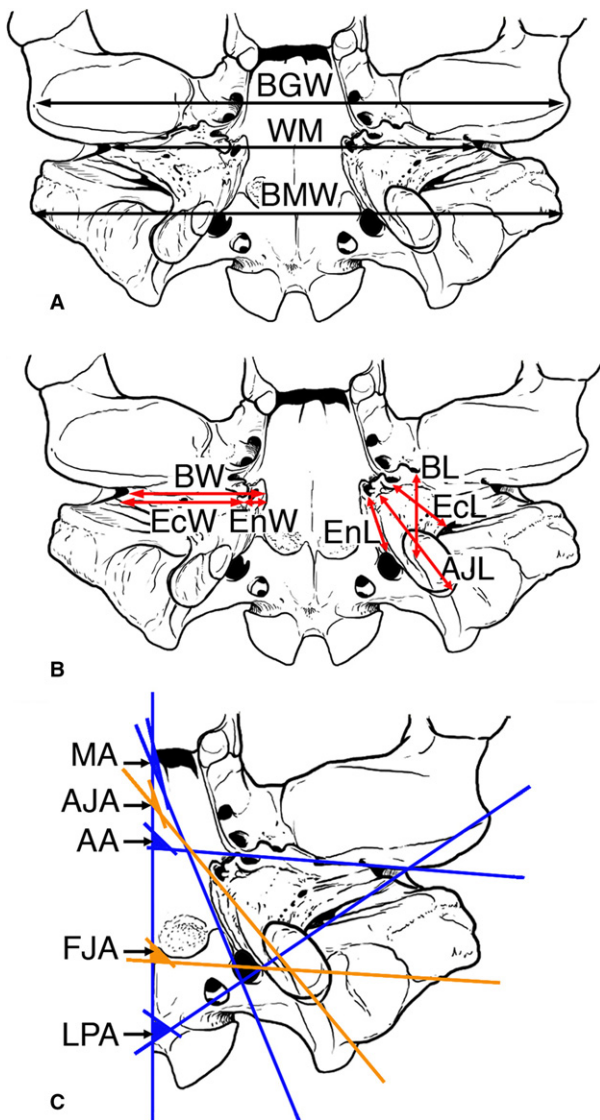
Fig. 1 Ventral views of the skull of *Otaria byronia*, showing measurements and angles (A,B) considered in this paper. (C) Detail of left bulla showing the angles. AA, anterior base angle; AJA, *Apophysis jugulare* angle; AJL, length of *apophysis jugulare;* BGW, biglenoid width; BL, maximum length of the bulla; BMW, bimastoid width; BW, maximum width of bulla; EcL, ectotympanic length; EcW, ectotympanic width; ENL, maximum length of endotympanic bone; EnW, endotympanic width; FJA, foramen jugulare angle; LPA, posterior base angle; MA, medial base angle; WM, width between meatuses.

Table 2 Cross-validated procedure over the known age specimens. Accuracy: 86.2069%.

	Bioclass I	Bioclass II	Bioclass III
Bioclass I	11	1	0
Bioclass II	1	11	4
Bioclass III	0	5	54

Table 3 Distribution of specimens between sex and age classes.

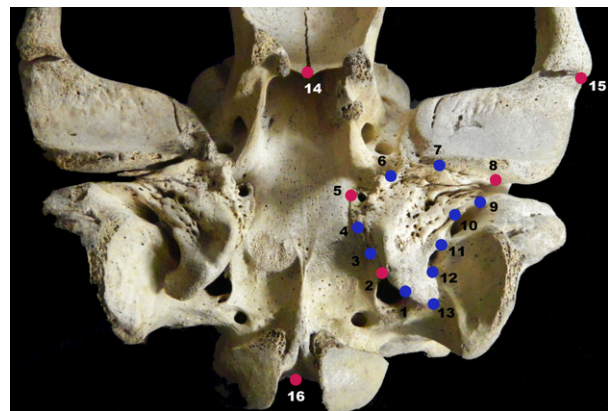|	Females	Males	Total
Bioclass I	9	3	12
Bioclass II	5	11	16
Bioclass III	22	37	59
Unknown age	52	62	114
Total	88	113	201

Fig. 2 Landmarks and semilandmarks used in the geometric morphometric analyses. purple, landmarks; blue, semilandmarks. Six homologous landmarks: Point 2, posteromedial contact between endotympanic and basioccipital; Point 5, anteromedial contact between endotympanic and basisphenoid; Point 8, most anteroventral point of the *meatus acusticus externus* where the retroarticular process of the glenoid cavity contacts the most anterolateral part of the ectotympanic; Point 14, most posterior contact point between palatines; Point 15, most lateral contact point between squamosal and jugal; Point 16, the midpoint on anterior border of the foramen magnum or basion. Additionally, 10 equidistant semilandmarks (Gunz & Mitteroecker, 2013) were placed along the outline of the tympanic bulla to capture its shape and curvature.

the landmark coordinates from all specimens to the average configuration (Berns & Adams, 2013). After superimposition, the aligned Procrustes shape coordinates were projected orthogonally into a linear tangent space, yielding Kendall's tangent space coordinates (Dryden & Mardia, 1998; Rohlf, 1999; Claude, 2008; Berns & Adams, 2013), which were treated as a set of shape variables for the exploration of shape variation. Centroid size was also retained for further analyses.

The digitizing process was performed using TᴘꜱDɪɢ2 (Rohlf, 2009) and morphometric analyses were performed in ʀ 3.3.2 (R Development Core Team, 2013), using routines in the package 'geomorph'

(Adams & Otárola-Castillo, 2013). Two approaches were used to assess possible sexual shape dimorphism and patterns of ontogenetic allometry. Initially, a principal components analysis (PCA) of the Procrustes coordinates was performed to visualize patterns of shape variation in the shape space. Second, a Procrustes ᴀɴᴏᴠᴀ with permutation was used statistically to assess possible shape differences between males and females, age classes and size (centroid size).

A regression of shape onto size was calculated and allometric patterns were visualized with a plot that describes the multivariate relationship between size and shape derived from landmark data. The abscissa of the plot is log (centroid size), whereas the ordinate represents shape, calculated as the common allometric component of the shape data (Mitteroecker et al. 2004; Adams & Nistri, 2010).

A cross-validated procedure was conducted in the 87 specimens separated into the three bioclasses to assess the robustness of the grouping criterion, with a resulting overall reclassification accuracy of 86% (Table 2).

Age classification of specimens with no absolute age data

Of the specimens included in the GM analysis (n = 201), 114 lacked information about absolute age. For between-group comparisons, in order to yield reliable results, it is important to increase the number of specimens per group (i.e. in each bioclass). Therefore, to be able to include specimens of unknown absolute age in subsequent analyses, we needed to define morphological classes (morphoclasses) for those specimens with known absolute age, which then allowed the inclusion of specimens of unknown age. For this, we used the morphology of the tympanic bulla defined by the scores of the PCA as a proxy for age class. Thus, the mean shape of the tympanic bulla of every bioclass was what defined the corresponding morphoclass.

The probability of a specimen of unknown absolute age falling within the multivariate normal distribution of one or more of the reference groups (morphological classes) is called typicality probability (Albrecht, 1992). This degree of similarity of the tympanic bulla of a specimen of unknown age to the reference groups is given by Mahalanobis distance, a value that best expresses the overall similarity of all variables between the test specimen and the reference group (Albrecht, 1992); the smaller the distance, the greater the similarity. Typicality probabilities are represented as values from 1 to 0; the higher the number, the more similar the values of the test specimen are to the mean of the reference sample. Typicality probabilities of less than 0.05 would indicate no affinity to the reference sample (Leach et al. 2009; Drake et al. 2015). Thus, typicality probabilities are the multivariate extension of the univariate t-test for evaluating whether a single observation belongs to a population. They are also the basis for evaluating whether an individual observation is an outlier with respect to a population (Albrecht, 1992, and references therein). The reference sample used is composed of the first 12 principal components of a PCA of the tangent space coordinates (retaining more than 95% of total shape variation) plus centroid size, since there is a significant association between shape and size (Fig. 3). The selected numbers of principal components were obtained using the Kaiser–Guttman criterion (Borcard et al. 2011). Typicality probabilities of specimens with no morphoclass were calculated using the MORPHO package (Schlager, 2016), following Wilson's (1981) method.

Results

Here we highlight the main features of ear anatomy in the homologous regions in different age classes of *O. byronia*, and analyze ontogenetic and sexual differences.
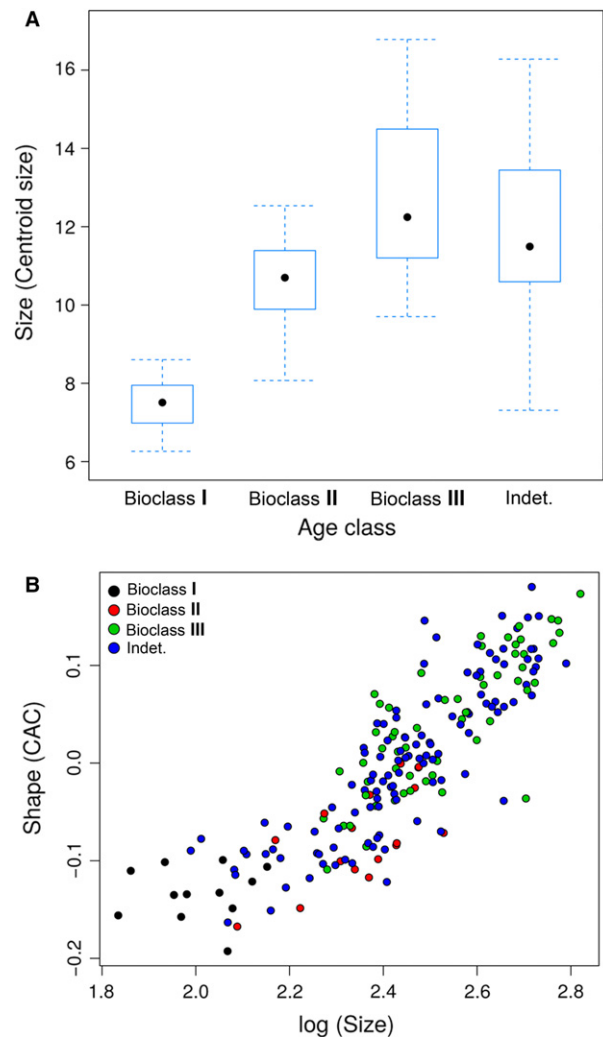

Fig. 3 (A) Box and whisker plot of size (centroid size) in each age class. (B) Regression of shape and size.

External morphology of the tympanic region

The mean shape of the bulla in *O. byronia* has a subtriangular contour, although it varies between males and females and between different ages. The surface is irregular and rugose, with some variation related to sex and ontogenetic stage.

In all cases, the ectotympanic is larger than the endotympanic, as in other otariids, and in contrast to *M. leonina* and other phocids (Loza et al. 2015). The suture between both bones is well defined in bioclass I and bioclass II, whereas in bioclass III it becomes covered by surface growth of the ectotympanic.

Foramina

Meatus acusticus externus (MAE): of moderate size with respect to the remaining foramina and to the entire skull, although it is the largest foramen with respect to

the condylobasal length of the skull, as well as to the bimastoid width (BMW) and the maximum width of the bulla (BW; Fig. 4). It is larger in males than in females, and also larger than that of *Arctocephalus*. It presents a mainly circular contour and is located laterally between the glenoid cavity and the *processus mastoideus* (PM) but it is medially displaced, and does not form a tubular structure as in *M. leonina*. Some differences can be observed in the distinct age classes (e.g. progressive closure of its floor by the ectotympanic; progressive elongation of the *meatus acusticus externus*) (Fig. 4A,C).

Sulcus tubae auditivae (STA) (or external foramen of the Eustachian tube *sensu* Pocock, 1916): the anterior aperture of the middle ear cavity, continuous with the Eustachian tube; it is small relative to the other foramina, and usually the smallest in diameter. It is comparatively smaller in males, and also smaller relative to the condylobasal length, bimastoid width, and maximum width of the bulla. This structure is even smaller in *Arctocephalus* spp. In other carnivores, *e.g.* procyonids, hyaenids, and ursids, it is called the 'anterior aperture of the auditory tube' (see Ivanoff, 2001) (Fig. 4B).

Anterior foramen of the *canalis caroticus* (CCAF), or *foramen lacerum*: located behind the alisphenoid, a ramus of the internal carotid passes through this foramen (Fig. 4A,B). In this species the anterior foramen of the *canalis caroticus* opens superficially at the base of the skull; it is apparent in palatal view and always well-developed. It is larger in females than in males. This foramen is known as 'foramen lacerum medium' in some mammals (*e.g.* Primates).

Posterior foramen of the *canalis caroticus* (CCPF): an opening posterior to the *canalis caroticus*, above the endotympanic, traversed by the carotid. This foramen is not always identified as such because in some other mammals it opens into a common vestibule with the *foramen jugulare*, leading to the former merging with the latter. However, it is always independent both in Phocidae and Otariidae, and especially conspicuous in the former. In *O. byronia* it shows a jagged contour and is proportionally larger in females than in males (Fig. 3A).

Foramen jugulare (FJ): the greater axis of this foramen is perpendicular to the sagittal plane (Fig. 4A), forming an angle that varies from 90° to 110°. It is located between the *bulla tympanica* and the occipital bone, traversed by the glossopharyngeal (IX), vagus (X), and accessory (XI) nerves, as well as the internal jugular vein, and corresponds to the *foramen lacerum posterior* of some authors (e.g. in Romer, 1949, for canids, ursids, and procyonids, and Hunt, 1974, for *Zalophus californianus*). It is proportionally smaller in *O. byronia* than in *Arctocephalus*, and smaller in females than in males. Its position is similar to that in other genera of otariids, such as *Eumetopias* and *Phocarctos* (as well as phocids),
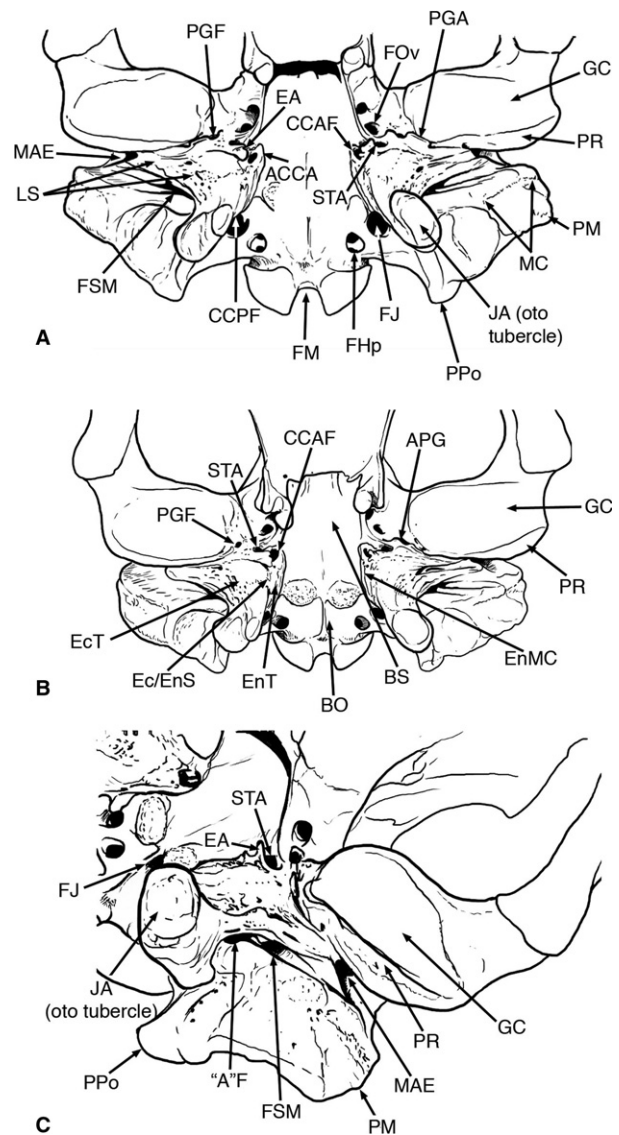

Fig. 4 Ventral views of the skull of *Otaria byronia*, showing the foramina and apophyses discussed in the text. (A) Ventral view, (B) anteroventral view, (C) posterolateral view. ACCA, anterior *canalis caroticus* anterior apophysis; 'A'F, A foramen; BO, basioccipital; BS, basisphenoid; CCAF, anterior foramen of the *canalis caroticus;* CCPF, posterior foramen of the *canalis caroticus;* EA, Eustachian apophysis; EcT, ectotympanic bone; Ec/EnS, ectotympanic–endotympanic suture; EnT, endotympanic bone; EnMc, endotympanic medial crest; FHp, *foramen hypoglossus;* FJ, *foramen jugulare;* FM, *foramen magnum;* FOv, *foramen ovale;* FSM, *foramen stylomastoideum;* GC, glenoid fossa; JA, *apophysis jugulare;* LS, lateral striae; MAE, *meatus acusticus externus;* MC, mastoid crests; PGA, postglenoid apophysis; PGF, postglenoid foramen; PM, *processus mastoideus;* PPo, *processus paraoccipitalis;* PR, *processus retroarticularis;* STA, *sulcus tubae auditivae.*

differing from that of some otariids such as *Arctocephalus*, *Neophoca*, *Callorhinus*, and *Zalophus*, where the foramen is parallel in orientation to the sagittal plane.

Foramen stylomastoideum (FSM): located postero-laterodorsal to the bulla, between the latter and the *processus mastoideus*; it is posterior to the *meatus acusticus externus* (Fig. 4C) and traversed by the facial nerve (VII) and the stylomastoid vein (which passes through the inner ear). It is always present and is one of the smallest foramina, being smaller in males than in females.

Foramen postglenoideum (PGF): posterior to the posteromedial angle of the glenoid cavity and anterior to the tympanic bulla. This foramen transmits the external jugular vein (Fig. 4A,B). It is markedly reduced or absent in most specimens, being one of the smallest foramina of the skull. It is larger in females than males, and usually larger than that of *Arctocephalus* spp.

Foramen 'A': located posterolateral to the *foramen stylomastoideum* (Fig. 4C); it may be evident and separated from the *foramen stylomastoideum*, merged with it, or simply be represented by a shallow depression (frequently obliterated in juveniles). Unlike the cases of other described foramina, it is proportionally larger in males than in females.

Foramen hypoglossus (FHp): close to the occipital condyles (thus it is also called 'condylar foramen') and the hypoglossal nerve (XII) passes through it. It is quite evident in most specimens, although in some it is merged with the *foramen jugulare* (Fig. 4A).

Regarding the openings in this area, the *canalis caroticus* is of moderate size with respect to other foramina of this cranial region, and smaller than its homologues in phocids. The *meatus acusticus externus* is small in comparison with cranial dimensions, but it is one of the largest foramina, with a greater diameter in males than in females, and it becomes proportionally longer as cranial width increases in males older than 5 years. Certainly, those differences are correlated with the ontogenetic trajectories of each sex. The *foramen stylomastoideum* is small and usually as large as the *meatus acusticus externus*. The *sulcus tubae auditivae* is one of the smallest in relative size, especially in males. Both the *sulcus tubae auditivae* and the *foramen stylomastoideum* are smaller than those of Phocidae. Finally, the *foramen postglenoideum* is also small but always present, in contrast to the observations in
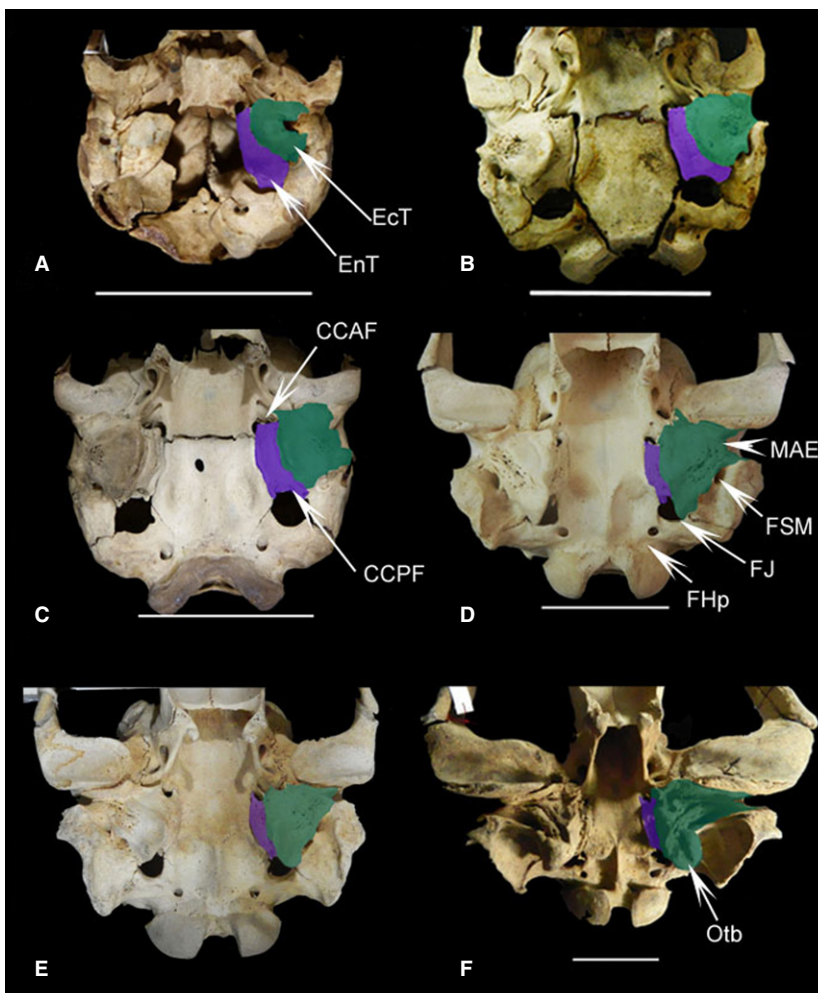

Fig. 5 External morphology of the tympanic bulla of *Otaria byronia* showing the differences in the development of the ectotympanic (green) and endotympanic (purple) bones in different morphological classes: morphoclass 1 (A and B), morphoclass 2 (C, female and D, male), morphoclass 3 (E, female and F, male).

phocids, in which the *foramen postglenoideum* is usually absent or very reduced. The homology of the 'A' foramen is doubtful, corresponding either to the vagal foramen or to a deviation of the *foramen stylomastoideum* (given that the 'A' foramen is associated with the *foramen stylomastoideum* in all specimens), as observed in phocids.

Apophyses

Although the tympanic bulla presents a variable shape and irregular surface, a basic morphological pattern can be discerned. The largest and most noticeable feature is the *apophysis jugulare* (AJ) (Figs 4–6), oriented anteromedially to posterolaterally, and clearly distinguishable from the first postnatal stages. However, its morphology does not perfectly match the term 'apophysis', as it is formed by a low crest (with a rounded profile) anteriorly and a taller structure posteriorly (with a sharp profile projected over the endotympanic).

In a more detailed analysis, it can be divided into two sections, described here as crests of the *apophysis jugulare* (AJ): an anterior crest (JAa), which is smaller and similar in both sexes, and a posterior one (JAp), whose morphology varies according to sex and age of the specimen. The posterior crest of the *apophysis jugulare* is extremely variable and may become a projection, which we refer to as ototubercle (Figs 4–6), which is the most evident crest on the surface of the tympanic bulla. The posterior crest of the *apophysis jugulare* increases in length, width and height along successive age classes, especially in males.

Surrounding anteriorly the *canalis caroticus* and located over the base of the occipital region, a lamina of the ectotympanic projects anteriorly as an apophysis (ACCA) (Fig. 4A). Posteriorly, there is another apophysis around the *canalis caroticus* (ACCP), smaller than the former, fused to the base of the skull, and covered by the ectotympanic, although it may be absent in some specimens.

Surrounding the *sulcus tubae auditivae* ventrally, the Eustachian apophysis (EA) has a variable shape, from prominent and spiky to flat-triangular, but also bifurcated and elongated (Fig. 4A).

The postglenoid apophysis (PGA) is transversely extended across the width of the glenoid cavity, but it may be restricted to a medial position (Fig. 4A).

A rounded stylomastoid apophysis (SMA) may be present, flanking the stylomastoid canal.

Finally, the *processus mastoideus* (PM) is large, with ornamentations and crests that vary across sex and age, and the *processus paraoccipitalis* (PPo) is very small or absent (possibly fused to the *processus mastoideus*, losing its independence and creating a compact, massive, and complex structure) (Fig. 4C).

Morphological classes and sexual dimorphism

Based on the mean shape of the tympanic bulla of the 87 specimens with known absolute ages (see GM results), three morphological classes may be clearly recognized:

Morphoclass 1 (corresponding to bioclass I): The ectotympanic varies from the typical horseshoe-shape, since in most cases it is not completely laterally closed (and does not close the base of the *meatus acusticus externus*), but when it is fused it forms a complete base of the *meatus acusticus externus* laterally (Fig. 5A,B, morphoclass 1).
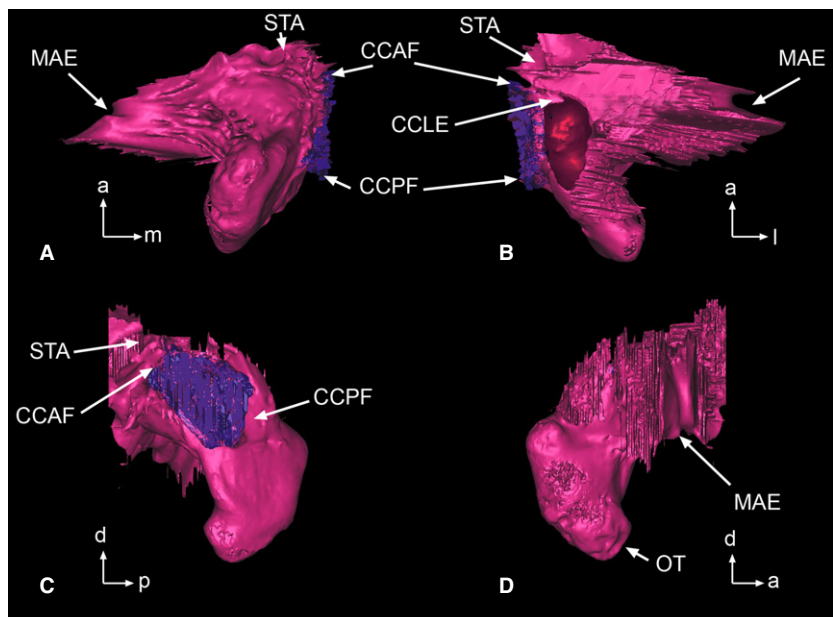
Fig. 6 Isolated tympanic bulla, generated by 3D reconstruction of the CT of an adult male of morphoclass 3 showing internal and external anatomy: (A) ventral view, (B) dorsal view, (C) medial view, and (D) lateral view. A, anterior; CCAF, anterior foramen of *canalis caroticus;* CCLE, lateral extension of *canalis caroticus;* CCPF, posterior foramen of *canalis caroticus;* D, dorsal; L, lateral; M, medial; MAE, *meatus acusticus externus;* OT, ototubercle; P, posterior; STA, *sulcus tubae auditivae.*

Morphoclass 2 (corresponding to bioclass II, sexually immature juveniles/subadults): The auditory bulla presents a smooth surface, quadrangular contour, and a laterally complete ectotympanic that also encircles the *meatus acusticus externus*. An incipient postglenoid apophysis, Eustachian apophysis, and posterior crest of the *apophysis jugulare* (JAp) may also be present (Fig. 5C, morphoclass 2).

Morphoclass 3 (corresponding to bioclass III): individuals with subtriangular *tympanic bullae* showing an irregular surface, bearing crests and processes that become noticeable, more in males than in females (Fig. 5D–F).

The morphological differences observed in specimens of each class involve multiple structures (Fig. 5D–F). The relative size of the ectotympanic varies. In morphoclass 1 this bone is horseshoe-shaped (with the opening oriented laterally) and has the least extension relative to the endotympanic; its lateral extreme is not complete and overlies (in ventral view) the lateralmost part of the endotympanic; it does not present surface ornamentation or striae. The *meatus acusticus externus* is not closed on its ventral surface (Fig. 5A,B). Progressively, in subsequent ontogeny (from morphoclass 2 onward), the ectotympanic grows to cover the endotympanic, and slight striae appear transversely on its surface (Fig. 6A). At the same time, it expands laterally, forming the ventral surface of the *meatus acusticus externus* (Fig. 5C–E). In older specimens (morphoclass 3) this bone is extended medially and posteriorly, to cover most of the endotympanic ventrally, with only a small region of the latter remaining visible (Fig. 5F).

The extension of the endotympanic also varies; its external expression is inverse to that observed for the ectotympanic, and it becomes progressively less visible (from morphoclass 1–3) due to ventral overlapping of the ectotympanic from below (Fig. 5).

The *apophysis jugulare* presents a slight medial curvature on the ectotympanic in morphoclass 1, and progressively grows in all directions in morphoclass 2 and morphoclass 3, reaching its maximum complexity and size in males older than 7 years (Fig. 5F). It usually presents variations in shape and is always very irregular (Fig. 6).

As previously mentioned, in older individuals the *processus mastoideus* is large, with ornamentations and crests; in morphoclasses 1 and 2 it may not be evident, whereas in morphoclass 3 females it is clearly visible and may even match the external limit of the glenoid cavity (or even surpass it in males older than 7 years).

Sexual dimorphism in the external morphology of the tympanic region is clear in morphoclass 3. These differences include the direction and shape of the *apophysis jugulare* during its growth, which becomes fairly posterior and angled in females; and the oto-tubercle, which is globose and rounded, and grows in a defined lateral direction in males, in which the oto-tubercle becomes larger than in females. In addition to the greater development of all apophyses and of the *processus mastoideus* in older males,
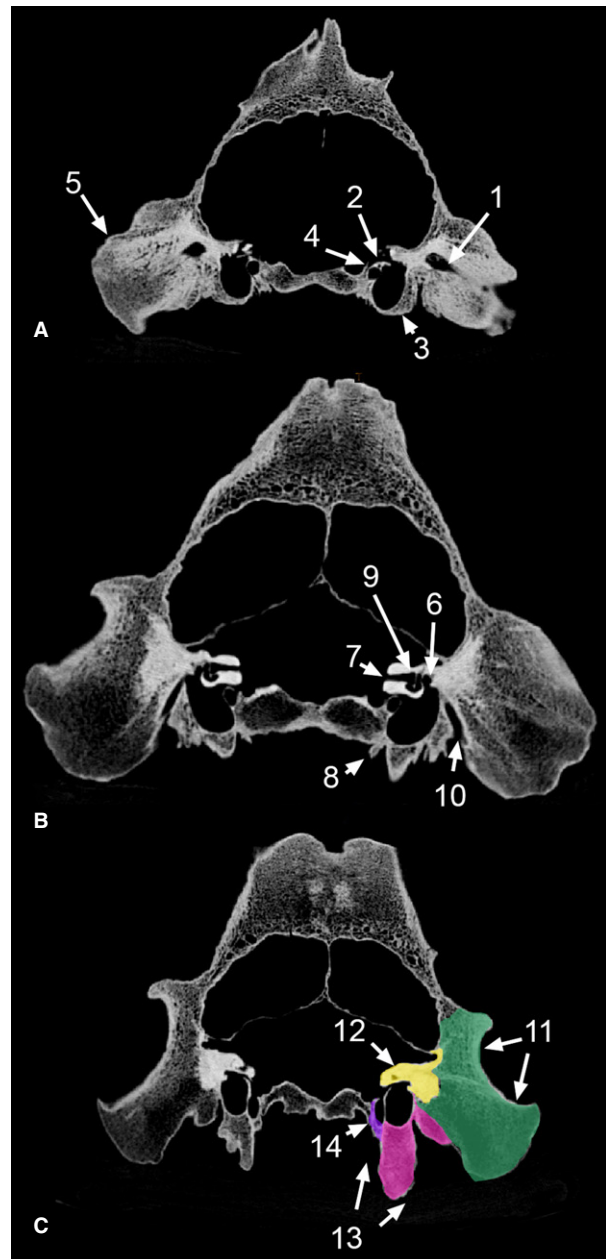
Fig. 7 Transverse views of a male morphoclass 3 specimen of *Otaria byronia*, showing three different sections in anteroposterior views of the variations along the auditory region: (A) anterior-most view; (B) middle view; (C) posterior-most view. 1: *meatus acusticus externus*; 2: lateral extension of *canalis caroticus*; 3: ectotympanic; 4: *canalis caroticus*; 5: mastoids; 6: *recessus epitympanicus*; *7: meatus acusticus internus*; 8: medial crest of endotympanic; 9: *cochlea*; 10: *foramen stylomastoideum*; 11: *pars escamosa* and *pars mastoidea*; 12: *pars petrosa*; 13: *pars tympanica*; 14: endotympanic.

the relative size of the ectotympanic compared with the endotympanic represents the greatest difference, as the ectotympanic entirely covers the endotympanic, especially on its posterior part that remains hidden underneath the *apophysis jugulare*.

The *processus mastoideus* is hardly differentiated until morphoclass 3, when it is clearly recognizable, and reaches the external limit of the glenoid cavity (in morphoclass 3) or even surpasses it.

Internal morphology

In *O. byronia* the mammalian temporal complex (which includes the otic region) involves a *pars petrosa*, a *pars tympanica*, a *pars escamosa* (like the corresponding ones observed in *M. leonina*), and a *pars mastoidea*. The latter is clearly recognizable from the *pars petrosa* by its lower bone density, and from the *pars escamosa* by a clearcut suture (Figs 7 and 8).

The middle ear of mammals comprises three sections, namely, the *annexae mastoidae*, the *cavum tympani*, and the Eustachian tube, or *Tuba pharingotympanica*

(Thomsassin et al. 2008); however, the first of these is absent in *O. byronia*, despite the large size of the *pars mastoidea*.

The endotympanic has two bifurcations, one anterior and one posterior; it is proportionally less extended than the ectoympanic, and thin-walled, narrower in its middle zone, and forming a ventrally oriented medial endotympanic crest (MEnC) (Fig. 7B).

The ectotympanic is the bone with the most variable morphology through ontogeny. It is relatively small and horseshoe-shaped in morphoclass 1, and expands peripherally in all directions, almost completely overlying the endotympanic. In internal view, the ectotympanic also projects as a lamina, extending over the ventral portion of the *pars mastoidea* and participating in the formation of the *processus mastoideus.* Throughout ontogeny, the ectotympanic progressively grows ventrally in several directions: anteriorly, to form the postglenoid and Eustachian apophyses; medially,

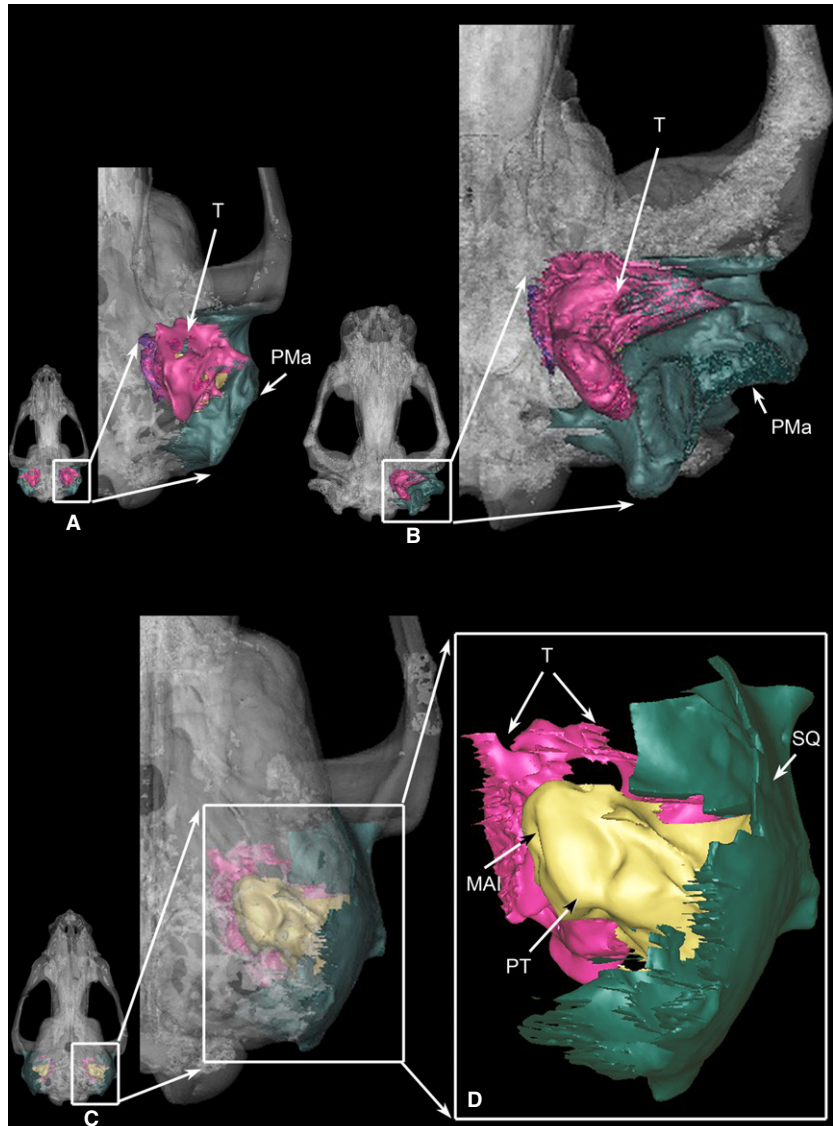**Fig. 8** Skulls of *Otaria byronia* (morphoclass 3) female and male, showing the general dimorphism and particularly the sexual dimorphism of the otic region. (A) Ventral view of a female skull, (B) ventral view of a male skull, (C) dorsal view of a female skull, (D) detail of the isolated otic region, showing the 3D structure of the three parts constituting it. PMa, *processus mastoideus;* PT, petrosal; SQ, squamosalal; T, tympanic.
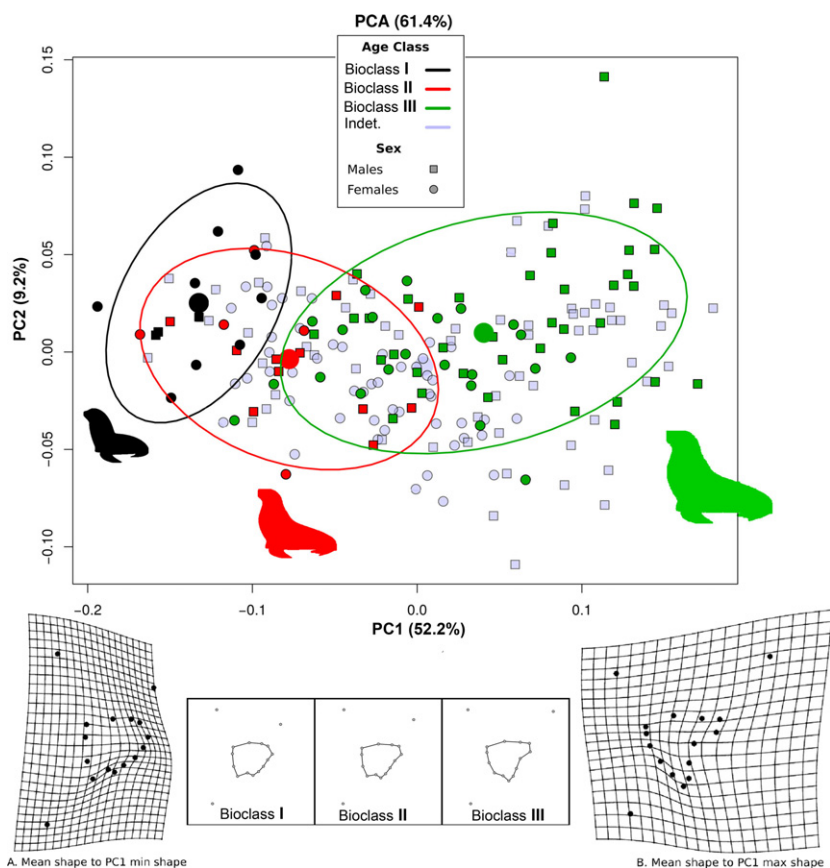
Fig. 9 Above, the PCA of the tangent space coordinates, showing the three bioclasses (bioclass I in black; bioclass II in red; bioclass III in green); and the individuals of unknown age (light gray). In the bottom middle, the mean shape of the tympanic bulla in the three bioclasses, called here morphoclasses. Bioclass I corresponds to morphoclass 1, bioclass II corresponds to morphoclass 2, bioclass III corresponds to morphoclass 3. In the bottom laterals, deformation grids of the extreme morphologies in the PCA.

Table 4 ANOVA table (Type I, sequential, significance testing by RRPP 10 000 permutations) for sex and age class.

	Df	SS	MS	Rsq	*F*	*Z*	Pr(> *F*)
Age class	2	0.79367	0.39683	0.287124	44.0056	24.6373	1e-04
Sex	1	0.11877	0.11877	0.042966	13.1701	10.3437	1e-04
Age class: sex	2	0.09329	0.04665	0.033751	5.1728	4.6673	1e-04
Residuals	195	1.75847	0.00902				
Total	200	2.76420					

Df, degrees of freedom for each term; *F*, the *F* values for each model term; MS, the mean of squares for each term; *P*, the *P*-values for each term from resampling permutations; Rsq, the coefficient of determination for each model term; SS, the sums of squares for each term; *Z*, the standard deviates or *z*-scores.

to cover the endotympanic; laterally, over the mastoid and becoming fused to it; and posteriorly, forming the ototubercle (Figs 6and 7).

The tympanic cavity as a whole is proportionally smaller than the same cavity in *M. leonina* or even in other phocids.

Following Gray (1858), the six surfaces that circumscribe the *cavum tympani* of the tympanic bulla are:

Paries tegmentalis (roof): formed anteriorly by the ventral surface of the petrosal, with a small *recessus epitympanicus*; a lateral projection of the *canalis caroticus* is absent, the roof is completed posteriorly by the ectotympanic and partially by the endotympanic (Fig. 7).

Paries jugularies (floor): there is no *recessus hypotympanicus*. Only the floor of the cavity, which does not present distinguishable accidents, forms the *paries jugularies*.

Paries labyrinthica (medial wall): formed by the lateral wall of the *canalis caroticus*, as in *M. leonina*, due to the dorsal position of the petrosal (Fig. 7B).

Paries mastoideus (posterior wall): does not have mastoid cells in any ontogenetic stage.

Paries carotica (anterior wall): delimited by an osseous Eustachian tube or *tuba pharingotympanica*, which is transversely elongated.

Paries membranaceus (lateral wall): delimited by the *meatus acusticus externus*, with medium-sized

Table 5 *P*-values of mean shape pairwise comparison between bioclass and sex. Values in bold correspond to non-significant ($P > 0.05$) mean shape differences between correspondent groups.

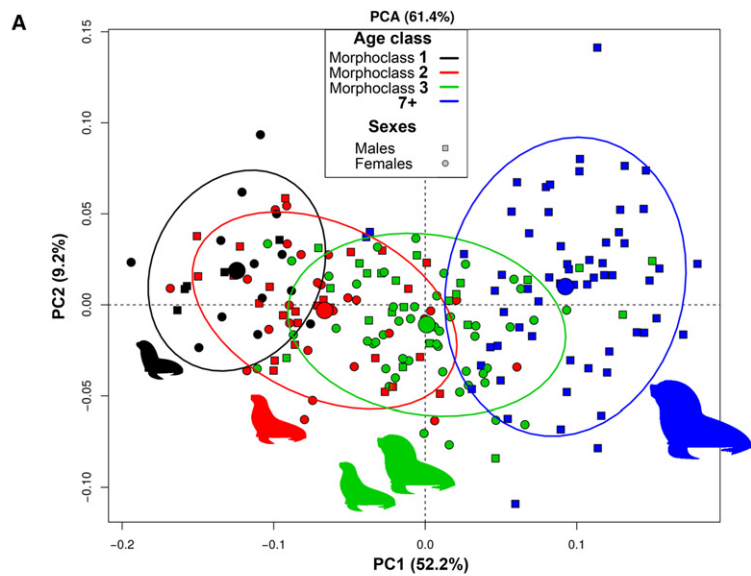|	Bioclass I: F	Bioclass I: M	Bioclass II: F	Bioclass II: M	Bioclass III: F	Bioclass III: M
Bioclass I: F	1	**0.4234**	0.0006	0.0002	0.0001	0.001
Bioclass I: M	**0.4234**	1	0.0035	0.0021	0.0001	0.001
Bioclass II: F	0.0006	0.0035	1	**0.0596**	0.0002	0.0106
Bioclass II: M	0.0002	0.0021	**0.0596**	1	0.0001	0.0001
Bioclass III: F	0.0001	0.0001	0.0002	0.0001	1	0.0077
Bioclass III: M	0.001	0.001	0.0106	0.0001	0.0077	1

Fig. 10 (A) PCA of the tangent space coordinates, showing the three morphoclasses (morphoclass 1 in black; morphoclass 2 in red; morphoclass 3 in green) and individuals 7 years old or older in blue. (B) Sequence of the tympanic region growth in different specimens, showing its ontogenetic transformation.

diameter in both sexes and all ages; the only change observed is progressive lengthening coincident with cranial growth. The *meatus acusticus externus* is oriented anteromedially from the *cavum tympani*, ending laterally in a posterolateral acoustic pore, differing from the ventral position of this pore in *M. leonina*.

The internal anatomy of the tympanic region does not show large differences between sexes and age classes, although the bullar volume is proportionally smaller compared with that of phocids.

Geometric morphometrics results

The first two principal components (PC1, PC2) explained 61.4% of the total shape variation, and showed several distinct clusters of specimens (Fig. 9). The different bioclasses are clearly identified, but with some degree of overlap. The deformation grids (Fig. 9) display the shape of the tympanic bulla at the ends of the range of variability along PC1, showing in the positive extreme a marked compression of the middle-posterior region of the tympanic bulla compared with a negative extreme of the PC1. Significant shape differences were found between both sexes and age classes (sequential type I Procrustes ANOVA with permutation, 10 000 iterations; $P < 0.05$). The interaction term was also significant ($P < 0.05$), indicating a combined effect of factors (sex and age stage) on morphology (Table 4). Regressions of shape vs. centroid size reveal a significant influence of allometry ($P < 0.05$), indicating size influences shape of the tympanic bulla.

Consequently, a model comparison was done to control the effect of size on sex and age classes. The models *shape ~ size*, and *shape ~ size + sex * age class* were compared and a pairwise comparison matrix constructed (Table 5).

The results showed that, although there were differences between males and females of different age classes, the only significant differences in tympanic bullar morphology occurred between males and females of bioclass III. Therefore, sexual dimorphism exists only between males and females of bioclass III, after accounting for size (Fig. 10).

Discussion

The structure of the bulla in otariids is more complex than in other pinnipeds such as phocids and odobenids, as well as other generalized carnivores such as felids and canids. Among southern otariids, *O. byronia* has the most extreme sexual dimorphism (Crespo, 1984; Jefferson et al. 2008). In agreement with these studies, our analysis of the otic region during ontogeny of both males and females showed extreme dimorphism.

One of the most noticeable features is the multidirectional growth of the ectotympanic during ontogenesis. From morphoclass 1 to morphoclass 3, the ectotympanic becomes progressively more prominent with respect to the endotympanic, and ends up covering it almost completely. Additionally, it also grows over the mastoid. A remarkably developed endotympanic is characteristic of phocids, whereas the ectotympanic is predominant in otariids (Berta et al. 2015).

The most conspicuous apophysis, characteristic of this species, is the *apophysis jugulare,* which forms a rounded oto-tubercle. This apophysis is incipient in morphoclass 1 and morphoclass 2, but is well defined in morphoclass 3, reaching its maximum size in morphoclass 3 males. In other species of otariids there is a projection homologous to the oto-tubercle that varies in shape; it may be a posteriorly directed cylindrical digitiform projection (e.g. in *Phocarctos hookeri*), an inverted triangle (e.g. in *Eumetopias jubatus*) or have a quadrangular outline (e.g. in *Zalophus californianus*). Although the morphology of the *apophysis jugulare* exhibits slight variations within each species (e.g. *P. hookeri* and *Z. californianus*), in *O. byronia* this variation reaches its greatest expression, and the apophysis and the oto-tubercle grow in different directions, adopting varied orientations and morphologies.

This apophysis shows a high degree of dimorphism in morphoclass 3, in males older than 7 years, and it is the region with the most ontogenetic changes (Fig. 10).

Both neonates and young pups are grouped in a well-defined morphoclass 1; this may be due to slower maturation in comparison with phocids, as otariids have a longer time span of parental care (Riedman, 1990).

The bulla does not increase in thickness through ontogeny, as in Phocidae; CT scans also show the extremely thin walls of adult specimens (as in generalized carnivores), differing from the condition in *M. leonina* and other phocids (*Lobodon, Hydrurga* or *Leptonychotes*) (see Loza et al. 2015). Coincidently, the Phocidae that present

a thick-walled bulla are those with records of diving at greater depths and for longer periods of time (Campagna et al. 1995, 1998, 1999, 2007; McIntyre et al. 2010a,b), whereas dives deeper than 200 m are unknown for *O. byronia* (Werner & Campagna, 1995; Thompson et al. 1998).

In *O. byronia* the external ornamentations of the bullar wall increase across these classes (from morphoclass 1 to morphoclass 3) but do not contribute to bullar thickness; the bullar wall is thin in all morphoclasses.

As shown in Fig. 11, the allometric trends of the bulla in males and females are convergent, the rate of change in males is higher (higher slope) and their ontogenetic trajectory surpasses that of females (Fig. 11A), leading to a greater change in size and shape (Fig. 11B). This heterochronic shift of males, when compared with females, results in a peramorphic condition, which is probably achieved by hypermorphosis (Chemisquy, 2015). The dashed lines in Fig. 11(A,B) highlight the value of the
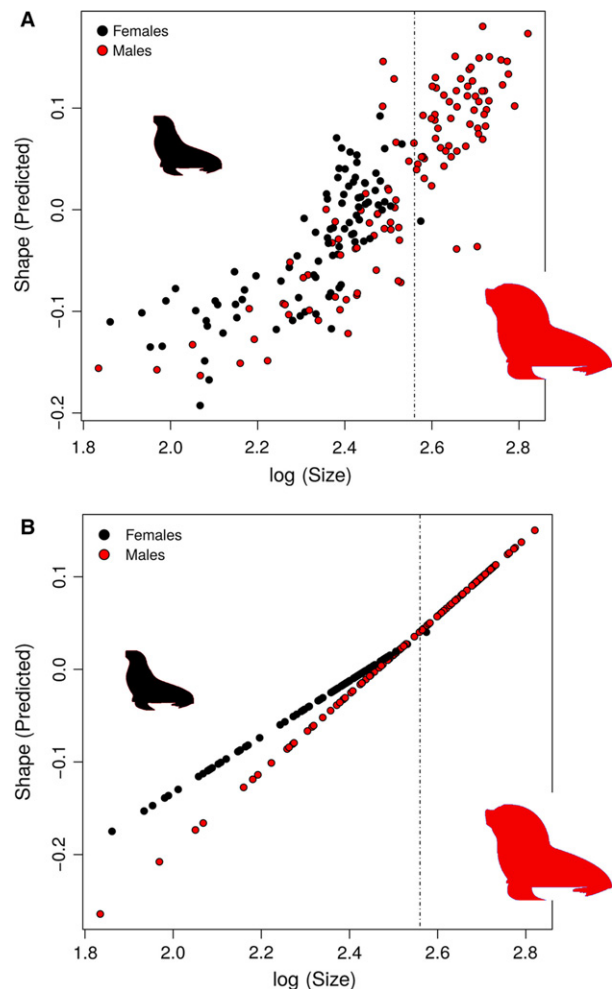

Fig. 11 Allometric trends of males and females showing the multivariate relationship between size and shape. (A) The common allometric component (CAC) vs. size (log centroid size). (B) Stylized trend following Adams & Nistri (2010). Dashed line indicates the minimum centroid size of 7-year-old males.

minimum centroid size of the males 7 years and older. This value clearly marks a threshold above which males exceed female growth. An important breakpoint where dimorphism becomes evident seems to happen when males pass the 7-year mark. Around this age, males undergo allometric growth (hypermorphosis) of the skull in general (Tarnawsky et al. 2014), which directly affects the structure of the otic region. At the same time, adult males areable to fight over harems and actually win these contests. Younger adult males that have not yet undergone these hypermorphic changes are prone to lose confrontations and remain as peripheral males outside the harems (Reyes et al. 1999). One example of the association between allometric growth of the skull and increasing ability to fight might be the exacerbated growth of the *processus mastoideus* and *apophysis jugulare*. These bony structures act as attachment surfaces for powerful neck muscles; head movements are used by males during fights to overcome the adversary.

Finally, as the tympanic region of *M. leonina* has previously been described and compared with other Phocidae (Loza et al. 2015), we describe and compare the same region of *O. byronia* with that of other Otariidae. It seems to be clear that the tympanic area of both *M. leonina* and *O. byronia* could be considered morphological models for their respective families, Phocidae and Otariidae. As we have shown here, each of these families can be defined using anatomical features of this region, and certain anatomical observations may agree with ecological aspects of the studied species (e.g. thickness of the wall of the bulla, which is greater in species that dive to greater depths).

Acknowledgements

References

Adams DC, Nistri A (2010) Ontogenetic convergence and evolution of foot morphology in European cave salamanders (Family: Plethodontidae). *BMC Evol Biol* **10**, 216.

Adams DC, Otárola-Castillo E (2013) Geomorph: an R package for the collection and analysis of geometric morphometric shape data. *Methods Ecol Evol* **4**, 393–399.

Adams DC, Rohlf FJ, Slice DE (2004) Geometric morphometrics: ten years of progress following the 'revolution'. *Ital J Zool* **71**, 5–16.

Adams DC, Rohlf FJ, Slice DE (2013) A field comes of age: geometric morphometrics in the 21st century Hystrix. *Ital J Mamm* **24**, 8.

Albrecht G (1992) Assessing the affinities of fossils using canonical variates and generalized distances. *Hum Evol* **7**, 49–69.

Arnaudo ME, Soibelzon LH, Bona P, et al. (2014) First description of the auditory region of a Tremarctine (Ursidae, Mammalia) Bear: the case of *Arctotherium angustidens*. *J Mamm Evol* **21**(3), 321–330.

Beaumont G (1968) Note sur la region auditive de quelques Carnivores. *Arch Sci Genéve* **21**, 211–224.

Berns CM, Adams DC (2013) Becoming different but staying alike: patterns of sexual size and shape dimorphism in bills of hummingbirds. *Evol Biol* **40**, 246–260.

Berta A, Sumich JM, Kovacs KM (2015) *Marine Mammals Evolutionary Biology*. 3rd edn., Amsterdam, Boston, Heidelberg, London, New York, Oxford, Paris, San Diego, San Francisco, Singapore, Sydney, Tokyo: Elsevier.

Bookstein FL (1996) Applying landmark methods to biological outline data. In: *Image Fusion and Shape Variability* (eds Mardia KV, Gill CA, Dryden IL), pp. 79–87. Leeds: University of Leeds Press.

Borcard D, Gillet F, Legendre P (2011) *Numerical Ecology with R*. New York, USA: Springer.

Brunner S, Bryden M, Shaughnessy PD (2004) Cranial ontogeny of otariid seals. *Syst Biodivers* **2**, 83–110.

Campagna C (1985) The breeding cycle of the southern sea lion, *Otaria byronia*. *Mar Mamm Sci* **1**, 210–218.

Campagna C, Le Bœuf BJ, Blackwell S, et al. (1995) Diving behaviour and foraging location of female southern elephant seals from Patagonia. *J Zool* **236**, 55–71.

Campagna C, Quintana F, Le Bœuf BJ, et al. (1998) Diving behaviour and foraging ecology of male southern elephant seals from Patagonia. *Aquat Mamm* **4**, 1–11.

Campagna C, Fedak MA, Mcconnell BJ (1999) Post-breeding distribution and diving behavior of adult male southern elephant seals fron Patagonia. *J Mamm* **4**, 1341–1352.

Campagna C, Piola AR, Maron MR, et al. (2007) Depp divers in shallow seas: Southern elephant seals on the Patagonia shelf. *Deep-Sea Res Part I* **54**, 1792–1814.

Canevari M, Vaccaro O (2007) Guía de mamíferos del sur de América del Sur. LOLA (Literature of Latin América).

Chemisquy MA (2015) Peramorphic males and extreme sexual dimorphism in *Monodelphis dimidiata* (Didelphidae). *Zoomorphology* **134**, 587–599.

Claude J (2008) *Morphometrics with R*. New York, USA: Springer.

Crespo EA (1984) Dimorfismo sexual en los dientes caninos y en los cráneos del lobo marino del sur, *Otaria flavescens* (Shaw) (Pinnipedia, Otariidae). *Rev Mus Argent Cienc Nat Bernardino Rivadavia* **25**, 245–254.

Crespo EA (1988) *Dinámica poblacional del lobo marino del sur Otaria flavescens* (Shaw, 1800), en el norte del litoral patagónico, p. 298. Buenos Aires: Facultad de Ciencias Exactas y Naturales, Universidad de Buenos Aires.

Crespo EA, Pedraza NS (1991) Estado actual y tendencia de la población de lobos marinos de un pelo *(Otaria flavescens)* en el litoral norpatagónico. *Ecol Austral* **1**, 87–95.

Cullen TM, Fraser D, Rybczynski N, Schröder-Adams C (2014) Early evolution of sexual dimorphism and polygyny in Pinnipedia. *Evol* **68**, 1469–1484.

Drake A, Coquerelle M, Colombeau G (2015) 3D morphometric analysis of fossil canid skulls contradicts the suggested domestication of dogs during the late Paleolithic. Scientific reports, p. 5.

Drehmer CJ, Ferigolo J (1997) Osteologia craniana comparada entre *Arctocephalus australis* e *Arctocephalus tropicalis* (Pinnipedia, Otariidae). *Iheringia Ser Zool* **83**, 137–149.

Dryden IL, Mardia KV (1998) *Statistical Shape Analysis*. Chichester: Wiley.

Flynn JJ, Finarelli JA, Zehr S, Hsu J, Nedbal MA (2005) Molecular Phylogeny of the Carnivora (Mammalia): Assessing the Impact of Increased Sampling on Resolving Enigmatic Relationships. *Syst Biol* **54**, 317–337.

Ginsburg L (1966) Les amphicyons des Phosphorites du Quercy. *Ann Paleontol* **52**, 23–64.

Gracham SF (1967) Seal ears. *Science* **155**, 48.

Grandi MF, Dans SL, García NA, et al. (2009) Growth and age at sexual maturity of South American sea lions. *Mamm Biol* **75**, 427–433.

Gray H (1858) *Gray's Anatomy, Descriptive and Surgical*. 15th revised edn. New York Toronto, London Sydney, Auckland: Gramercy Books, Random House Value Publishing.

Gunz P, Mitteroecker P (2013) Semilandmarks: a method for quantifying curves and surfaces. *Hystrix Ital J Mamm* **24**, 7.

Hough JR (1948) The auditory region in some members of the Procyonidae, Canidae, and Ursidae. Its significance in the phylogeny of the Carnivora. *Bull Am Mus Nat Hist* **92**, 67–118.

Hough JR (1952) Auditory region in North American Felidae: significance in phylogeny. *Geol Surv Prof Pap* **243**, 95–115.

Hunt RM Jr (1974) The auditory bulla in Carnivora: an anatomical basis for reappraisal of carnivore evolution. *J Morphol* **143**, 21–76.

Ivanoff DV (2000) Origin of the septum in the canid auditory bulla: evidence from morphogenesis. *Acta Theriol* **45**, 253–270.

Ivanoff DV (2001) Partitions in the carnivorian auditory bulla: their formation and significance for systematics. *Mamm Rev* **31**, 1–16.

Jefferson TA, Webber MA, Pitman RL (2008) *Marine Mammals of the World: A Comprehensive Guide to Their Identification*. Amsterdam, Boston, Heidelberg, London, New York, Oxford, Paris, San Diego, San Francisco, Singapore, Sydney, Tokyo: Academic Press, Elsevier.

King JE (1964) *Seals of the World*, pp. 125–126. London: British Museum (Natural History).

King JE (1983) *Seals of the World*. 2nd edn. Ithaca, NY: Cornell University Press.

Laws RM (1953) A new method of determination in mammals with special reference to elephant seal (*Mirounga leonina* L.). *Falkland Isl Depend Surv Sci Rep* **2**, 1–11.

Laws RM (1993) Identification of species. In: *Antarctic Seals: Research Methods and Techniques* (ed. Laws RM), pp. 1–28. Cambridge: Cambridge University Press.

Leach S, Lewis M, Chenery C, et al. (2009) Migration and diversity in Roman Britain: a multidisciplinary approach to the identification of immigrants in Roman York, England. *Am J Phys Anthropol* **140**, 546–561.

Loza CM (2016a) Morfología comparada y ontogenia del oído medio e interno en Pinnípedos (Otariidae y Phocidae, Carnivora) de la Argentina y Antártida. Aspectos ecomorfológicos. PhD Tesis. Universidad Nacional de La Plata, Buenos Aires, Argentina, pp. 496.

Loza CM (2016b) Nomenclatura osteológica y accidentes de la región ótica de pinnípedos y sinónimos. *Rev Mus La Plata* **1**, 117–158.

Loza CM, Scarano AC, Soibelzon LH, et al. (2015) Morphology of the tympanic-basicranial region in *Mirounga leonina* (Phocidae, Carnivora), postnatal ontogeny and sexual dimorphism. *J Anat* **226**, 354–372.

Loza CM, Soibelzon LH, Tarnawski BA, et al. (2016) Determinación de edades de Otariidae y Phocidae (Carnivora) sobre piezas dentarias, técnicas alternativas. *Rev Mus La Plata* **1**, 39–56.

Marsh SE (2001) Morphometric Analyses of ears in two families of the Pinnipeds. Ph.D dissertation, B.A, Rice University. Master of Science at The Massachusetts Institute of Technology and The Woods Hole Oceanographic Institution.

McIntyre T, De Bruyn PJN, Ansorge IJ, et al. (2010a) A lifetime at depth: vertical distribution of southern elephant seals in the water column. *Polar Biol* **33**, 1037–1048.

McIntyre T, Tosh CA, Plötz J, et al. (2010b) Segregation in a sexually dimorphic mammal: a mixed-effects modelling analysis of diving behaviour in southern elephant seals. *Mar Ecol Prog Ser* **412**, 293–304.

Mitteroecker P, Gunz P, Bernhard M, et al. (2004) Comparison of cranial ontogenetic trajectories among great apes and humans. *J Hum Evol* **46**, 679–697.

Mohl B (1967) Frequency discrimination in the common seal and discussion of the concept of upper hearing limit. In: *Underwater Acoustics*, vol. **2** (ed. Albers V), pp. 43–54. New York: Plenum Press.

Mohl B (1968) Auditory sensivity of the common seal in air and water. *J Acoust Res* **1**, 27–38.

Nummela S (1995) Scaling of the mammalian middle ear. *Hear Res* **85**, 18–30.

Odend'hal S, Poulter TC (1966) Pressure regulation in the middle ear cavity of the sea lions: a possible mechanism. *Science* **153**, 768–769.

Pocock RI (1916) The tympanic bulla in Hyenas. Proceedings of the Zoological Society of London. pp. 303–307.

Pocock RI (1921) The external characters and classification of the Procyonidae. *Proc Zool Soc Lond* **1921**, 389–422.

Pocock RI (1922) The external characters and classification of the Mustelidae. *Proc Zool Soc Lond* **91**, 803–837.

Pocock RI (1929) The structure of the auditory bulla in the Procyonidae and the Ursidae, with a note on the bulla of Hyaena. *Proc Zool Soc Lond* **98**, 963–974.

Ponce de León A, Pin OD (2006) Distribución, reproducción y alimentación del lobo fino *Arctocephalus australis* y del león marino *Otaria flavescens* en Uruguay. In: *Bases para la conservación y el manejo de la costa uruguaya*. (eds Menafra R, Rodríguez-Gallego L, Scarabino F, Conde D), pp. 1–9. Montevideo: Vida Silvestre, Sociedad Uruguaya para la Conservación de la Naturaleza.

R Development Core Team (2013). R: A Language and Environment for Statistical Computing. Version 3.0.2. Vienna: R Foundation for Statistical Computing.Available at: http://cran.R-project.org.

Reyes LM, Crespo EA, Szapkievich V (1999) Distribution and population size of the southern sea lion (*Otaria flavescens*) in Central and Southern Chubut, Patagonia, Argentina. *Mar Mamm Sci* **15**, 478–493.

Riedman M (1990) *The Pinnipeds: Seals, Sea Lions, and Walruses (No. 12)*. Berkeley and Los Angeles: University of California Press.

Rohlf FJ (1999) Shape statistics: Procrustes superimpositions and tangent spaces. *J Class* **16**, 197–223.

Rohlf RJ (2009) TPSDIG, version 2.12. Department of Ecology and Evolution, State University of New York, Stony Brook, NY (http://life.bio.sunysb.edu/morph/).

Rohlf FJ, Marcus LF (1993) A revolution in morphometrics. *Trends Ecol Evol* **8**, 129–132.

Rohlf FJ, Slice D (1990) Extensions of the Procrustes method for the optimal superimposition of landmarks. *Syst Zool* **39**, 40–59.

Romer AS (1949) *The Vertebrate Body*, p. 643. Philadelphia: Saunders Co.

Rosas FCW, Haimovici M, Pinedo MC (1993) Age and growth of the South American sea lion, *Otaria flavescens* (Shaw, 1800), in Southern Brazil. *J Mamm* **74**, 141–147.

Sanfelice D, De Freitas RO (2008) A comparative description of dimorphism in skull ontogeny of *Arctocephalus australis*, *Callorhinus ursinus* and *Otaria byronia*. *J Mamm* **89**, 336–346.

Schlager A (2016) Morpho: Calculations and visualisations related to geometric morphometrics. R package version 2.4.1.1. https://CRAN.R-project.org/package=Morpho

Solnsteva GN (1972) Comparative anatomical peculiarities of the middle ear structure in terrestrial, semi aquatic and aquatic mammals. Abstr. 5th All-Un Conf Mar Mamm Res Makhachkala **2**, 216–220 (In Russian).

Solnsteva GN (1973a) Biomechanical features of the middle ear in terrestrial, semi aquatic and aquatic mammals. Abstr. 8th All-Un Acoust Conf Moscow, **128**: 29–32.

Solnsteva GN (1973b) Morphological and biomechanic features of the middle ear of the Caspian seal (*Pusa caspica*). In Dolk. 74–76. Sessii Kasp NIRKH porabotam za 1972. Astrakhan.

Solnsteva GN (1975) Morphofunctional peculiarities of the auditory organ in terrestrial, semi aquatic and aquatic mam\mals. *Zool Zhurn* **44**, 1529–1539.

Tarnawsky BA, Cassini GH, Flores DA (2013a) Skull allometry and sexual dimorphism in the ontogeny of the southern elephant seal (*Mirounga leonina*). *Can J Zool* **92**(1), 19–31.

Tarnawsky BA, Cassini GH, Flores DA (2014) Allometry of the postnatal cranial ontogeny and sexual dimorphism in *Otaria byronia* (Otariidae). *Acta Theriol* **59**, 81–97.

Thenius E (1949) Zur Revision der Insektivoren des steirischen Tertiars II. *Sitzungsb Osterr Ak Wiss Math-naturwissensch Klas Abt I* **159**, 671–693.

Thompson D, Duck CD, McConnel BJ, et al. (1998) Foraging behavior and diet of lactating female southern sea lions (*Otaria flavescens*) in the Falkland Islands. *J Zool Lond* **246**, 135–146.

Thomsassin JM, Dessi P, Danvin JB, et al. (2008) Anatomía del oído medio. *EMC* (Elsevier Masson SAS,París) Oto-rhino-laryngologie, **37**(3), 1–20. DOI 20-015-A-10.

Van der Klaauw CJ (1930) On mammalian auditory bullae showing an indistinctly complex structure in the adult. *J Mamm* **11**, 55–60.

Van der Klaauw CJ (1931) The auditory bulla in some fossil mammals. *Bull Am Mus Nat Hist* **62**, 1–135.

Van Kampen PN (1905) Die Tympanalgegend des Saugetierschadels. *Morph Jb* **34**, 321–722.

Vaz-Ferreira R (1981) South American sea lion *Otaria flavescens* (Shaw 1800): 39-65 in: Ridgway & Harrison (1981).

Werner R, Campagna C (1995) Diving behaviour of lactating southern sea lions (*Otaria flavescens*) in Patagonia. *Can J Zool* **73**, 1975–1982.

Wilson S (1981) On comparing fossil specimens with population samples. *J Hum Evol* **10**, 207–214.

Wozencraft WC (1989) The phylogeny of the recent Carnivora. In: *Carnivore Behavior, Ecology, and Evolution* (ed. Gilttelman JL), pp. 495–535. New York, Cornell University Press.

Wozencraft WC (2005). Order Carnivora. In: *Mammal Species of the World* (eds Wilson DE, Reeder DM), 3rd edn, pp. 532–628. Baltimore: The Johns Hopkins University Press.

Wyss A (1987) The walrus auditory region and the monophyly of Pinnipeds. *Am Mus Novit* **2871**, 1–32.

Wyss A (1988) On 'Retrogression' in the evolution of the phocinae and phylogenetic affinities of the monk seals. *Am Mus Novit* **2924**, 1–40.

Zelditch M, Swiderski D, Sheets D, et al. (2004) *Geometric Morphometrics for Biologists*. Amsterdam: Academic Press, Elsevier.

Appendix 1

List of studied specimens, their Age Class (morphoclass), Sex, and Absolute age (determined by counting lines on sectioned teeth).

Collection	Age class	Sex	Absolute age
MACN 13.13	CIII	M	11
MACN 13.14	CIII	M	12
MACN 20420	CIII	M	6
MACN 20572	CIII	F	10
MACN 20573	CIII	F	8
MACN 20578	CIII	F	8
MACN 20579	CIII	F	NA
MACN 20583	CIII	M	NA
MACN 20595	CII	M	NA
MACN 20596	CIII	F	10
MACN 21737	CIII	F	7
MACN 21738	CIII	F	7
MACN 21739	CII	F	2
MACN 21742	CIII	F	NA
MACN 21743	CIII	M	5
MACN 21744	CII	M	4
MACN 21984	CIII	M	NA
MACN 21994	CIII	M	NA
MACN 21995	CIII	M	NA
MACN 22371	CIII	M	10
MACN 22608	CIII	F	11
MACN 22609	CIII	M	6
MACN 22851	CIII	M	NA
MACN 22852	CIII	M	5
MACN 22853	CIII	H	8
MACN 23.26	CIII	M	NA
MACN 24635	CIII	M	NA
MACN 24733	CIII	M	NA
MACN 24851	CIII	M	NA
MACN 24967	CIII	F	NA
MACN 24994	CII	F	NA
MACN 25.45	CIII	M	5
MACN 25102	CII	M	NA

Collection	Age class	Sex	Absolute age
MACN 25138	CIII	F	7
MACN 25168	CIII	M	NA
MACN 27.27	CIII	M	11
MACN 30236	CI	M	NA
MACN 41226	CIII	M	12
MACN 50.52	CIII	M	6
MACN 13.11	CIII	F	11
MCN 2460	CIII	M	NA
MCN 2462	CIII	H	NA
MCN 2505	CIII	M	7
MCN 2521	CIII	F	NA
MCN 2525	CIII	M	5
MCN 2526	CIII	M	NA
MCN 2528	CII	M	1
MCN 2533	CIII	F	NA
MCN 2601	CII	M	4
MCN 2602	CIII	M	5
MCN 2603	CIII	M	5
MCN 2604	CIII	F	11
MCN 2610	CII	M	4
MCN 2612	CIII	M	7
MCN 2616	CIII	M	5
MCN 2619	CII	M	2
MCN 2622	CII	M	3
MCN 2629	CIII	M	12
MCN 2686	CII	M	2
MCN 2691	CIII	F	7
MCN 2693	CIII	M	5
MCN 2695	CII	M	4
MCN 2696	CIII	M	6
MCN 2697	CIII	M	NA
MCN 2698	CII	F	NA
MCN 2700	CIII	M	NA
MCN 2701	CIII	F	NA
MCN 2703	CIII	M	5
MCN 2704	CIII	F	11
MCN 2806	CIII	M	17
MCN 2807	CIII	M	NA
MCN 2837	CIII	M	NA
MCN 2838	CIII	M	NA
MCN 2846	CIII	M	NA
MCN 2885	CII	M	1
MCN 2966	CII	F	NA
MCN 2990	CIII	M	NA
MLP 1060	CIII	F	7
MLP 1328	CIII	M	11
MLP 1330	CIII	M	13
MLP 1331	CIII	M	NA
MLP 1332	CIII	M	9
MLP 14.iv.48.9	CII	M	NA
MLP 1526	CIII	M	10
MLP 1531	CIII	F	6
MLP 1532	CIII	M	10
MLP 1886	CIII	F	12
MLP 1968	CIII	F	9

(continued)

Collection	Age class	Sex	Absolute age
MLP 2195	CIII	M	NA
MLP 2196	CIII	M	NA
MLP 26.iv.00.1	CIII	M	14
MLP 26.iv.00.10	CIII	M	10
MLP 26.iv.00.11	CIII	M	8
MLP 26.iv.00.2	CIII	M	8
MLP 26.iv.00.3	CIII	M	11
MLP 26.iv.00.4	CIII	M	NA
MLP 26.iv.00.5	CII	F	2
MLP 26.iv.00.8	CII	M	2
MLP 26.iv.00.9	CII	F	2
MLP 26.iv.02.34	CIII	M	10
MLP 27.X.97.14	CIII	F	NA
MLP 4.X.94.4	CIII	M	15
MLP 404	CIII	M	14
MLP 41	CIII	F	11
MLP 453	CIII	F	10
MLP 465	CIII	F	13
MLP 475	CIII	F	13
MLP 49	CIII	M	8
MLP 628	CII	F	3
MLP 7.VII.50.1	CII	F	4
MLP 8.X.01.8	CII	M	3
MLP 82	CIII	M	11
MNHN 5848	CI	M	NA
MNHN 6083	CI	F	NA
MNHN 6092	CIII	F	NA
MNHN 6095	CII	M	NA
MNHN 6104	CIII	F	NA
MNHN 6121	CII	F	NA
MNHN 6124	CII	M	NA
MNHN 6125	CII	M	NA
MNHN 6127	CII	F	NA
MNHN 6144	CIII	F	NA
MNHN 6167	CIII	M	NA
MNHN 6170	CII	M	NA
MNHN 6447	CIII	F	NA
MNHN 6448	CII	F	NA
MNHN 6453	CIII	M	NA
MNHN 6454	CIII	F	NA
MNHN 6710	CIII	M	NA
MNHN 6711	CIII	M	NA
MNHN 6714	CII	F	NA
MNHN 6930	CIII	M	NA
MNHN 6937	CIII	M	NA
MNHN 6938	CIII	M	NA
MNHN 6945	CIII	M	NA
MNHN 6946	CII	M	NA
MNHN 6947	CIII	F	NA
MNHN 6955	CIII	M	NA
MNHN 7087	CIII	F	NA
MNHN 7088	CIII	M	NA
MNHN 7216	CIII	F	NA
MNHN 7221	CIII	F	NA
MNHN 7358	CIII	F	NA

(continued)

Appendix 1 . (continued)

Collection	Age class	Sex	Absolute age
OF 101	CI	F	NA
OF 102	CI	F	NA
OF 103	CI	M	NA
OF 104	CII	M	NA
OF 106	CII	M	NA
OF 107	CII	F	NA
OF 108	CI	F	NA
OF 110	CI	F	NA
OF 115	CI	F	NA
OF 247	CIII	F	NA
OF 249	CI	F	NA
OF 270	CIII	M	NA
OF 274	CII	F	NA
OF 276	CII	M	NA
OF 290	CI	F	NA
OF 294	CI	F	NA
OF 301	CI	F	NA
OF 302	CI	F	NA
OF 304	CI	M	NA
OF 340	CIII	F	NA
OF 341	CIII	F	NA
OF 345	CIII	F	10
OF 48	CII	F	NA
OF 66	CI	F	NA
OF 68	CII	F	NA
OF 70	CI	F	NA
OF 87	CII	F	NA
UDELAR 331	CII	M	NA
UDELAR 1171	CII	F	NA

Appendix 1 . (continued)

Collection	Age class	Sex	Absolute age
UDELAR 1181	CIII	M	NA
UDELAR 1188	CIII	F	NA
UDELAR 1189	CIII	F	NA
UDELAR 1191	CIII	F	NA
UDELAR 1192	CIII	M	NA
UDELAR 1193	CIII	M	NA
UDELAR 1194	CIII	F	NA
UDELAR 1196	CII	F	NA
UDELAR 1525	CII	F	NA
UDELAR 1526	CII	F	NA
UDELAR 1581	CII	F	NA
UDELAR 1586	CII	F	NA
UDELAR 2132	CIII	M	NA
UDELAR 2236	CII	F	NA
UDELAR 2237	CIII	F	NA
UDELAR 28	CIII	M	NA
UDELAR 29	CIII	M	NA
UDELAR 332	CII	F	NA
UDELAR 360	CIII	F	NA
UDELAR 46	CI	M	NA
UFSC 1055	CII	F	NA
UFSC 1134	CIII	M	NA
UFSC 1140	CIII	M	NA
UFSC 1152	CIII	M	NA
UFSC 1161	CIII	M	NA
UFSC 1162	CII	M	NA
UFSC 1168	CIII	M	NA
UFSC 1171	CIII	M	NA
UFSC 1341	CII	M	NA